Supporting Information

Amphoteric molecular Engineering of the Buried SnO_2/Perovskite Interface toward Efficient and Durable Solar Cells

Qingquan He[a,b], *Yu Bao*[a], *Shicheng Pan*[a], *Tao Zhang*[a], *Xinquan Wang*[a], *Yaxuan Yang*[a], *Qingyue Guo*[a], *Jijin Qiao*[a], *Jing Li**[a,b], *and Jun Pan**[a,b]

a. Science and Education Integration College of Energy and Carbon Neutralization, College of Materials Science and Engineering, Zhejiang Provincial Key Laboratory of Clean Energy Conversion and Utilization, State Key Laboratory of Green Chemical Synthesis and Conversion, Zhejiang University of Technology, Hangzhou 310014, P. R. China.

b. Zhejiang Baima Lake Laboratory Co., Ltd., Hangzhou 310000, Zhejiang, P. R. China.
Email: qqhe21@zjut.edu.cn, lijing23@zjut.edu.cn, panjun0123@zjut.edu.cn

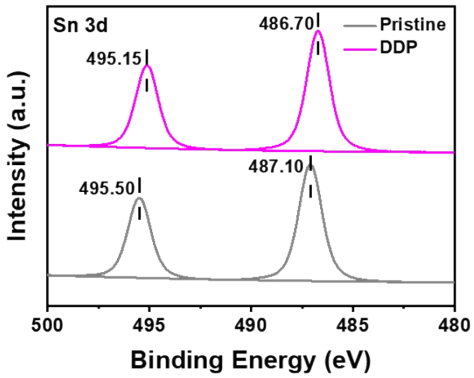

Fig. S1 XPS spectra of Sn 3d of SnO_2 and SnO_2/DDP ETLs.

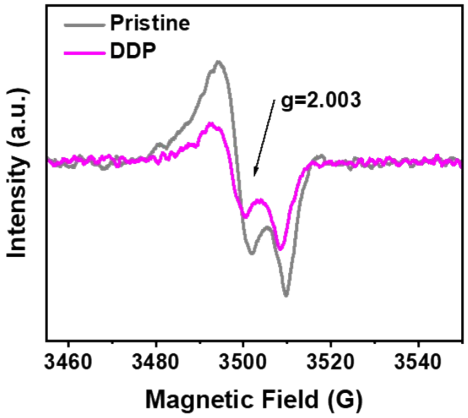

Fig. S2 Electron paramagnetic resonance (EPR) spectra of pristine and DDP-modified SnO_2 films.

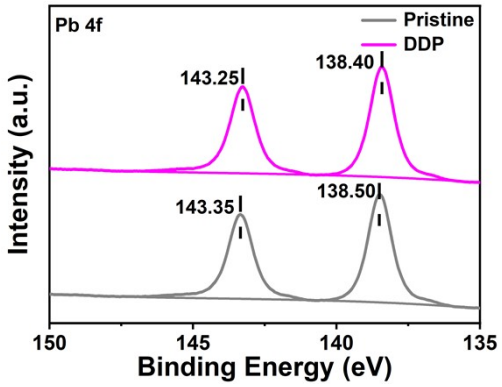

Fig. S3 XPS spectra of Pb 4f for the top surface of pristine and DDP-modified perovskite films.

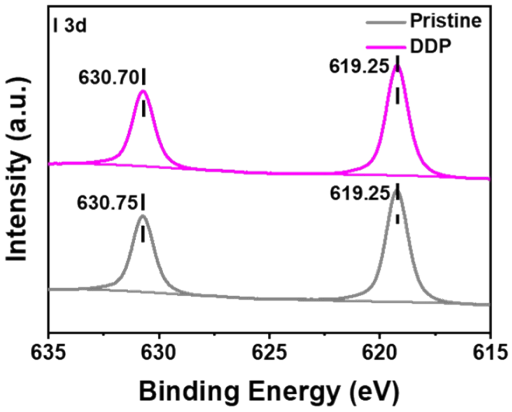

Fig. S4 XPS spectra of I 3d for the top surface of pristine and DDP-modified perovskite films.

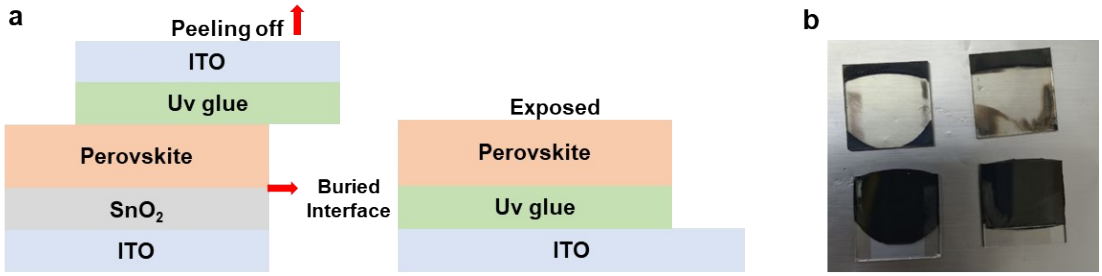

Fig. S5 (a) Schematic diagram of perovskite films peeling from ITO/SnO_2 substrate. (b) Photograph of peeled-off perovskite films.

UV-curable adhesive was applied onto the perovskite thin film. The ITO glass was then carefully placed flatly on top of the perovskite thin film, ensuring the uniform distribution of the UV-curable adhesive. Subsequently, the adhesive was cured under UV light irradiation for 1 minute. The PVK thin film with the UV-curable adhesive could then be peeled off from the ITO/SnO_2 substrate.

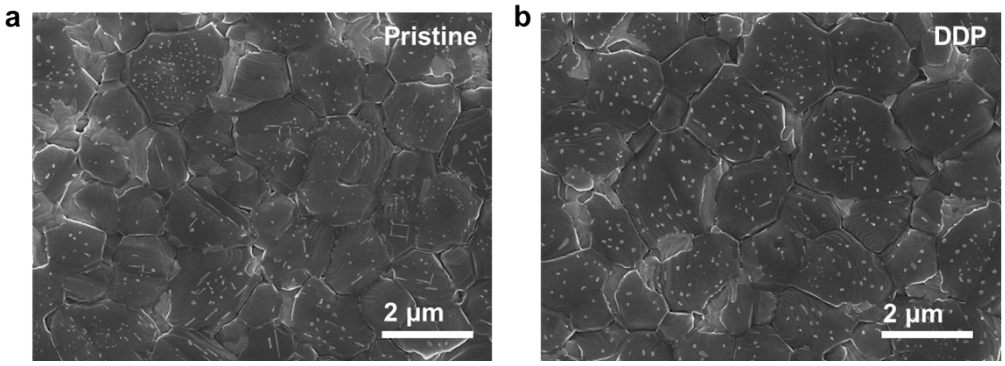

Fig. S6 SEM images of the top surface of the (a) pristine and (b) DDP-modified perovskite films.

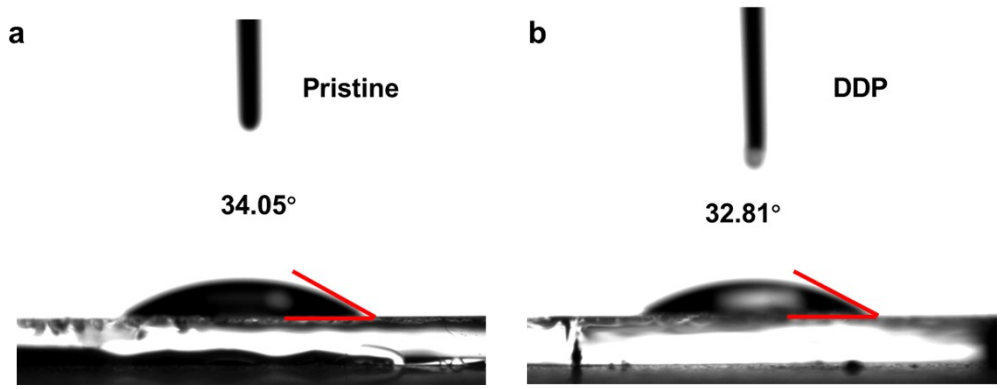

Fig. S7 Water contact angle of the (a) pristine and (b) DDP-modified perovskite films.

Table S1. Fitting parameters of the TRPL spectra of pristine and DDP-modified perovskite films

Samples	**τ_1 (ns)**	**τ2 (ns)**	**τ_{avg} (ns)[a]**
Pristine	498.3	4174.7	3654.9
DDP	1.9	333.5	333.3

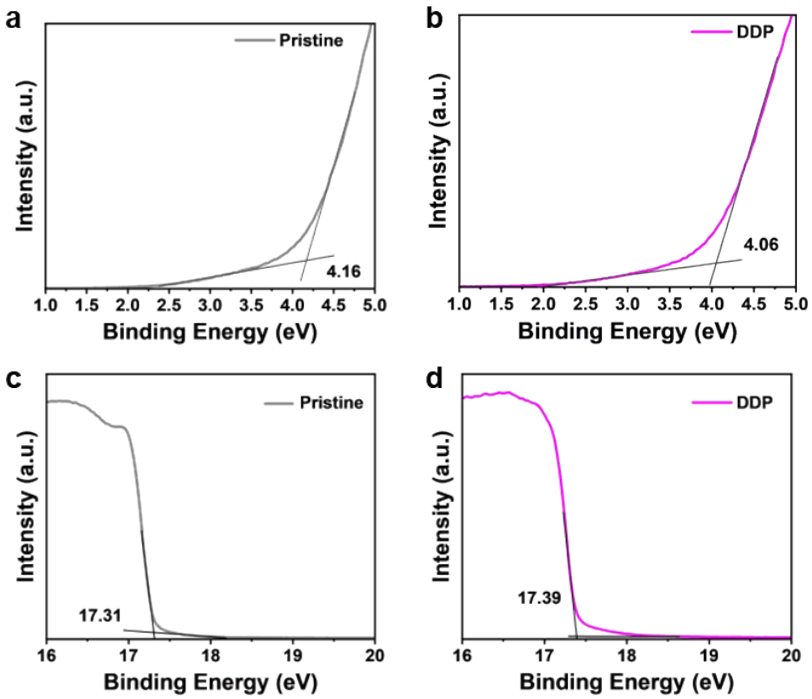

Fig. S8 The starting region (a, b) and the cutoff region (c, d) of the ultraviolet photoelectron spectroscopy of the (a, c) SnO_2 and (b, d) SnO_2/DDP ETLs.

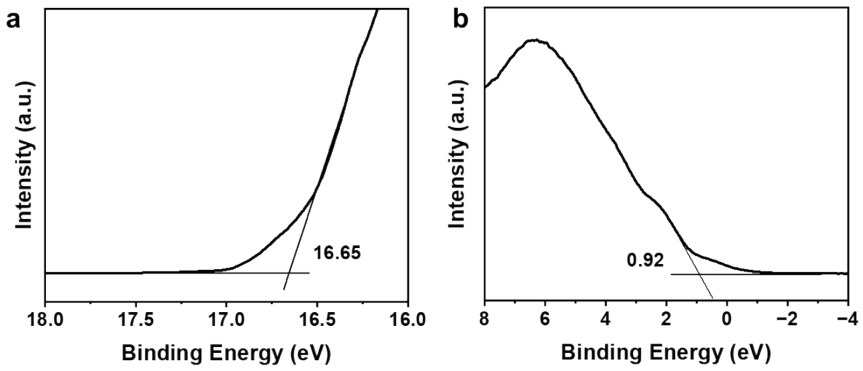

Fig. S9 UPS energy spectra in (a) onset and (b) cut-off regions of perovskite film.

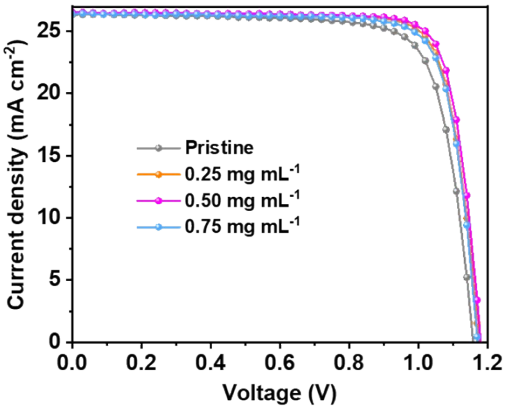

Fig. S10 J-V curves of the champion devices based on DDP-modified perovskite films at different concentrations.

Table S2. Photovoltaic parameters of the DDP-modified PSCs with various concentrations

Sample		J_{SC} (mA·cm^{-2})	V_{OC} (V)	FF (%)	PCE (%)
DDP	0 mg mL^{-1}	26.34	1.158	77.44	23.63
	0.25 mg mL^{-1}	26.49	1.174	80.75	25.13
	0.50 mg mL^{-1}	26.55	1.180	81.51	25.54
	0.75 mg mL^{-1}	26.39	1.171	80.02	24.73

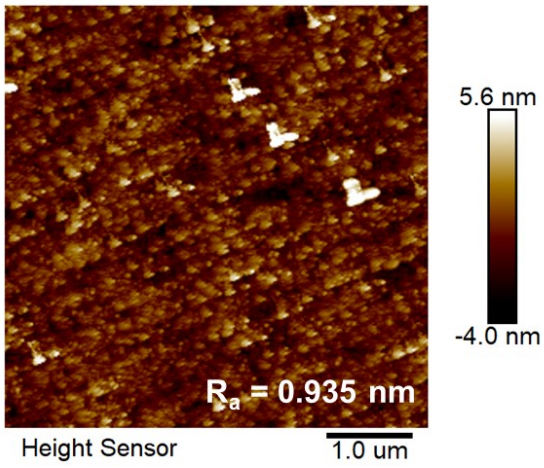

Fig. S11 AFM image of the SnO_2 ETL modified with 0.75 mg mL^{-1} DDP.

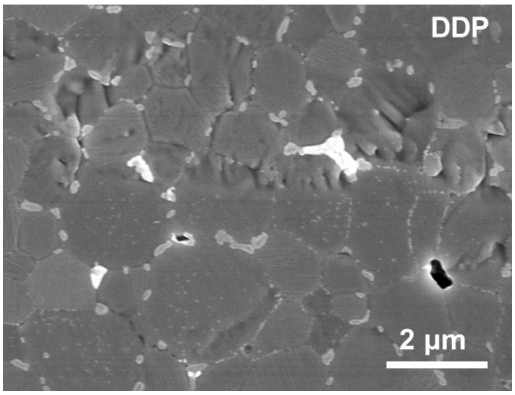

Fig. S12 SEM image of the bottom surface of perovskite films modified with 0.75 mg mL^{-1} DDP.

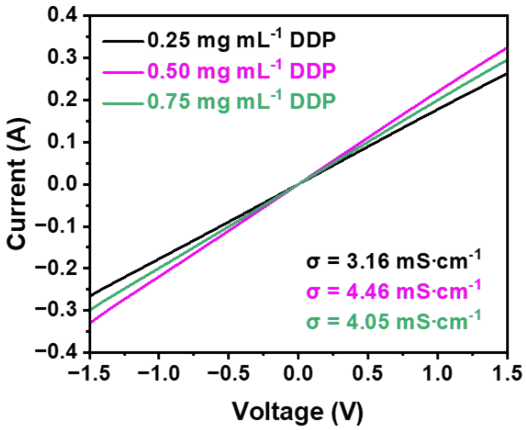

Fig. S13 Electrical conductivity of the SnO_2/DDP film modified with 0.25, 0.50 and 0.75 mg mL^{-1} DDP.

Table S3. Photovoltaic parameters of the pristine and DDP-modified champion devices

Sample	Direction	J_{SC} (mA·cm^{-2})	V_{OC} (V)	FF (%)	PCE (%)
Pristine	Reverse	26.34	1.158	77.44	23.63
	Forward	26.48	1.134	72.94	21.92
DDP	Reverse	26.55	1.180	81.51	25.54
	Forward	26.47	1.163	77.28	23.80

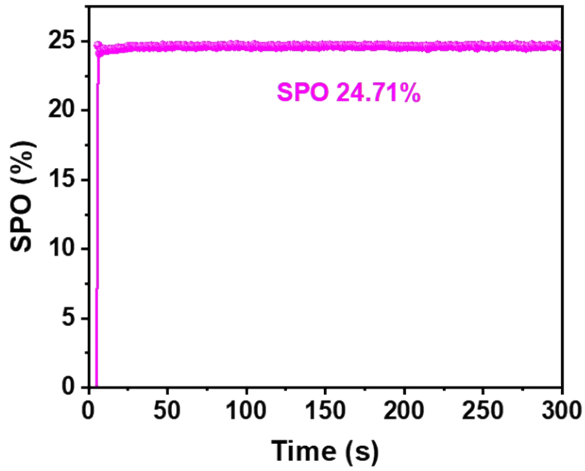

Fig. S14 Stabilized power output (SPO) of the DDP-modified device.

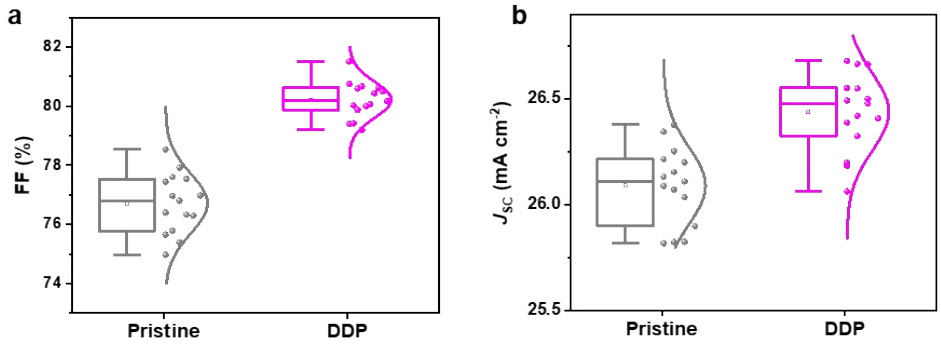

Fig. S15 Statistical distributions of (a) FF and (b) J_{SC} for PSCs based on the pristine and DDP-modified perovskite films.